Hennadii V. Pavlov
Павлов Геннадий Викторович

Andrii V. Obrubov
Обрубов Андрей Валерьевич

Mykhailo V. Pokrovskyi
Покровский Михаил Владимирович

Iryna L. Vinnychenko
Винниченко Ирина Леонидовна

УДК 621.314
П12

ELECTROMAGNETIC PROCESSES IN THE POWER SECTION OF THE SERIES-TO-SERIES RESONANT CONVERTER FOR CONTACTLESS INDUCTIVE ENERGY TRANSFER

ЭЛЕКТРОМАГНИТНЫЕ ПРОЦЕССЫ В СИЛОВОЙ ЧАСТИ ПОСЛЕДОВАТЕЛЬНО-ПОСЛЕДОВАТЕЛЬНОГО РЕЗОНАНСНОГО ПРЕОБРАЗОВАТЕЛЯ ДЛЯ БЕСКОНТАКТНОЙ ИНДУКТИВНОЙ ПЕРЕДАЧИ ЭЛЕКТРОЭНЕРГИИ

DOI 10.15589/SMI20170214

Hennadii V. Pavlov Г. В. Павлов, д-р. техн. наук, проф.
gennadiy.pavlov@nuos.edu.ua
ORC ID: 0000-0002-4937-1828

Andrii V. Obrubov А. В. Обрубов, канд. техн. наук, доц.
andrii.obrubov@nuos.edu.ua
ORC ID: 0000-0001-9667-1703

Mykhailo V. Pokrovskyi М. В. Покровский, канд. техн. наук, доц.
mykhailo.pokrovskyi@nuos.edu.ua
ORC ID: 0000-0002-6851-3748

Iryna L. Vinnychenko И. Л. Винниченко, преп.
i.l.vinnychenko@gmail.com
ORC ID: 0000-0002-3768-1060

Admiral Makarov National University of Shipbuilding, Nikolaev
Национальный университет кораблестроения имени адмирала Макарова, г. Николаев

Abstract. The paper analyzes the electromagnetic processes in the power section of the series-to-series resonant converter for contactless inductive energy transfer. Static characteristics or the converter are discussed. The state-variable method has been implemented to solve the vector-matrix equations describing the processes in the power section of the converter, which allowed obtaining the dependence of the average value of the output current on the parameters of the circuit elements, the load, and the size of the transformer gap. There have been also obtained the load and adjustment characteristics of the converter. The research results can be applied in the development of a converter control system. The adjustment characteristics are established for a sufficiently large interval with a large air gap; they are of a linear form. The load characteristics are quite rigid, which simplifies control of the converter's output current.

Keywords: two-circuit resonant converter; contactless energy transfer; state-variable method; static characteristics.

Аннотация. Проанализированы электромагнитные процессы в силовой части последовательно-последовательного резонансного преобразователя для бесконтактной индуктивной передачи энергии. Получены решения векторно-матричных систем уравнений, описывающих электромагнитные процессы в силовой части резонансного преобразователя для бесконтактного электропитания. Получена зависимость среднего значения выходного тока преобразователя от параметров элементов резонансных контуров, величины воздушного зазора трансформатора, параметров источника и нагрузки. Построены статические характеристики последовательно-последовательного резонансного преобразователя.

Ключевые слова: двухконтурный резонансный преобразователь; бесконтактная передача энергии; метод переменных состояния; статические характеристики.

Анотація. Проаналізовано електромагнітні процеси в силовій частині послідовно-послідовного резонансного перетворювача для безконтактної індуктивної передачі енергії. Отримані рішення векторно-матричних систем рівнянь, що описують електромагнітні процеси в силовій частині резонансного перетворювача для безконтактного електроживлення. Отримано залежність середнього значення вихідного струму перетворювача від параметрів елементів резонансних контурів, величини повітряного зазору трансформатора, параметрів джерела і навантаження. Побудовано статичні характеристики послідовно-послідовного резонансного перетворювача.

Ключові слова: двоконтурний резонансний перетворювач; безконтактна передача енергії; метод змінних стану; статичні характеристики.

References

[1] Pokrovskiy M. V. *Posledovatelno-rezonansnye preobrazovateli postoyannogo napryazheniya s releynym regulirovaniem* [Series-resonant DC converters with relay control]. PHD dissertation. Kyiv, 2006. 159 p.

[2] Pavlov G. V., Scherbinin T. V. *Sravnenie kharakteristik rezonansnykh preobrazovateley razlichnykh topologiy s ispolzovaniem imitatsionnykh modeley* [Comparison of the characteristics of resonant converters of various topologies using simulation models]. Tekhnichna elektrodynamika [Technical Electrodynamics]. Kyiv, 2012, no. 2, pp. 57–58.

[3] Rudenko V. S., Senko V. I., Chizhenko I. M. *Osnovy preobrazovatelnoy tekhniki* [Fundamentals of converting equipment]. Moscow, High School Publ., 1980. 418 p.

[4] Scherbinin T. V. *Osobennosti impulsnykh transformatorov v rezonansnykh preobrazovatelyakh dlya beskontaktnoy induktivnoy zaryadki akkumulyatorov elektrotransporta* [Special features of pulse transformers in resonant converters for contactless inductive charging of electric vehicle's batteries]. *Tekhnichna elektrodynamika. Tematichnyi vypusk «Sylova elektronika ta energoefektyvnist»* [Technical Electrodynamics. Special issue "Power Electronics and Energy Efficiency"]. Kyiv, 2012, vol. 4, pp. 81–86.

[5] Kobayashi K., Pontefract T., Kamiya Y., Daisho. Y. Development and Performance Evaluation of a Non-contact Rapid Charging Inductive Power Supply System for Electric Micro-bus. *IEEE Vehicle Power and Propulsion Conference (VPPC)*, 2011, pp. 1–6.

[6] Mecke R., Rathge C. High frequency resonant inverter for contactless energy transmission over large air gap. *IEEE Power Electronics Specialists Conference*, 2004, vol. 3, pp. 1737–1743.

[7] Pavlov G., Obrubov A., Vinnichenko I. The linearized dynamic model of the series resonant converter for small signals. 2016 *2nd International Conference on Intelligent Energy and Power Systems (IEPS)*. Kyiv, 2016, pp. 1–5.

[8] Valtchev S., Borges B., Klaassens B. Series Resonant Power Converter for Contactless Energy Transfer with Improved Efficiency. UTL-IST (Portugal), TU Delft (the Netherlands), 2008. 402 p.

[9] Wang Ch.-S., Stielau O., Covic G. Design considerations for a contactless electric vehicle battery charger. *IEEE Transactions on Industrial Electronics*, 2005, vol. 52, no. 5, pp. 1308–1314.

Problem statement. Autonomous electronic devices of small and medium power capacity that require periodic battery recharging are widely represented among portable communication devices, office equipment, in medicine, automotive industry, etc. However, the fact that conventional conductive power supply interfaces feature friction contacts reduces the reliability of the devices, limiting their use or making it completely unacceptable, as is the case with electronic implants. For this reason, contactless energy transfer systems are being actively developed; they make use of an inductive coupling for energy transmission over certain distances. In the presence of a large air gap, such systems are characterized with a low magnetizing inductance and high dissipated inductances. The use of resonance converters in this case will reduce switching losses, increase the conversion frequency and efficiency, and improve the conditions for electromagnetic compatibility. It will also effectively compensate for the impact of dissipated inductances, providing for a high output power of the converter with a large air gap.

Latest research and publications analysis. The output power capacity of the inductive transmission is inversely proportional to the size of the air gap and directly proportional to the conversion frequency [6]. Therefore, the use of resonant converters providing soft switching of power keys allows achieving a greater power capacity of the magnetic system without increasing the dynamic loss in the keys [1 – 3, 7]. At that, the magnetizing and dissipated inductances will become part of the resonant circuit connected to the output of the inverter [4]. If resonant capacitors of such ratings are included to the circuits of the transmitter coil and the receiver coil, the circuits will be tuned to the same resonant frequency, and the efficiency of the inductive transmission will be increased substantially [5, 8, 9].

A series-to-series topology of resonant converters (RC) is similar to a series-to-parallel RC but with the resonant circuit containing two inductors [2]. The series connection of the resonant capacitor on the rectifier side endows the converter with the properties of a constant voltage source [9]. The main advantage of this topology is the ease of calculating the resonant capacitor on the inverter side; the inverter rating should be selected only with account for the desired resonance frequency and the values of the dissipated inductances and the capacitor's rating on the rectifier side [8, 9].

THE ARTICLE AIM is to study the electromagnetic processes in the power section of a series-to-series resonant converter for contactless inductive energy transfer and obtain its static characteristics.

Basic material. The use of resonant converters providing soft switching of power keys allows achieving a greater power of the magnetic system without increasing the dynamic loss in the keys. Taking into account the advantages of the series-to-series RC topology for contactless inductive energy transmission, it is advisable to use a converter with the power section of a layout shown in Fig. 1.

The device consists of two parts. The ground part contains a power factor corrector (PFC), a high-frequency inverter (I), a series resonant circuit (RCir1), and a magnetic coil used as a transmitter antenna. The mobile part includes a receiver coil, a series resonant circuit (RCir2), a rectifier with a filter (Rec) and a load (L). Energy transmission occurs through the magnetic coupling between the receiver and transmitter coils. A circuit diagram of the power section of the RC for wireless inductive energy transmission (WIET) is shown in Fig. 2.

Pulse-count adjustment offers such advantages as the minimal dynamic loss, possibility of maintaining a switching frequency equal to the resonant frequency over the whole range of adjustment, and maintenance of a sinusoidal current. These features make it the most attractive option of the adjustment of the output current in resonant converters.

In the case of pulse-count adjustment, the adjustment cycle consists of n_{FrRv} half- cycle s of resonance oscillations of the ***Fr*** and ***Rv*** conversion phases and n_{Ds} half-cycles of the ***Ds*** conversion phase. The duration of each half-cycle is equal to $T_{osc}/2$. The total number of half-cycles is $n = n_{FrRv} + n_{Ds}$. Each half-cycle of resonant oscillations can be conveniently divided into intervals during which energy is transmitted in one direction. These intervals are dubbed as *conversion phases* [1]. The conversion phases characteristic of the series-to-series RC are shown in Fig. 3.

Two phase types can be distinguished within the conversion half-cycle. During the direct conversion phase ***Fr***, energy is transmitted from the source to the load. During the reverse conversion phase ***Rv***, the energy of the circuit is partially recovered to the source and partially transmitted to the load. Thereat, the difference in the currents flowing through the primary winding dissipated inductance and magnetizing inductance $I_{Ld1} - I_{Lm} = I_{Ld2}$ changes its sign, which leads to an increase in the current of the load. The I_{Ld1} current then flows towards the EMF of the source. Within this phase, the conditions are created for power transistors switching at zero voltage. In the course of the circuit energy dissipation, there is only one conversion phase ***Ds*** (the energy accumulated in the circuit is dissipated to the load). Equivalent circuits of the series-to-series RC for the conversion phases under consideration are given in Table 1.

Let us compose the state equations for the power section of the resonant converter with a series connection of the capacitors of the primary and secondary circuits. The controlled variable is the converter's output current $y(t) = i_m(t) = i_{Ld2}(t)$, the controlling variable is the number of voltage pulses in the loading phase n_{FrRv}. The processes occurring in the resonant circuit are characterized with the state vector $x^T(t) = [i_{Ld1}(t)\ i_{Lm}(t)\ u_{Cd1}(t)\ u_{Cd2}(t)]$.

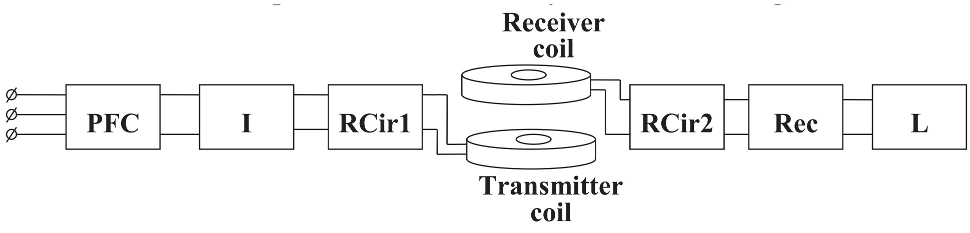

Fig. 1. Block diagram of the power section of the RC for wireless inductive energy transmission

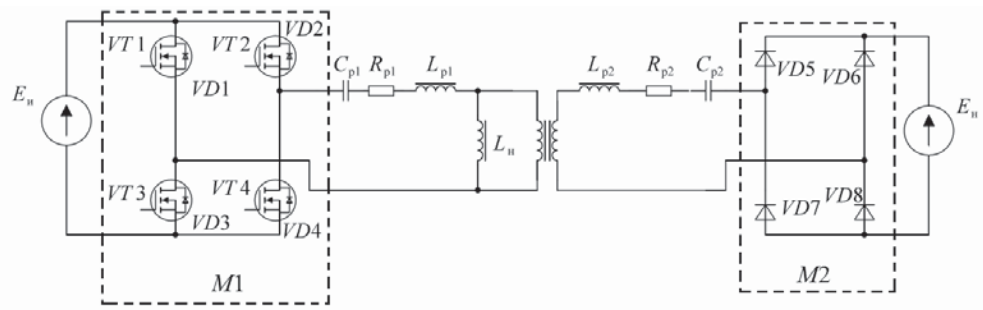

Fig. 2. Circuit diagram of the power section of the RC for WIET

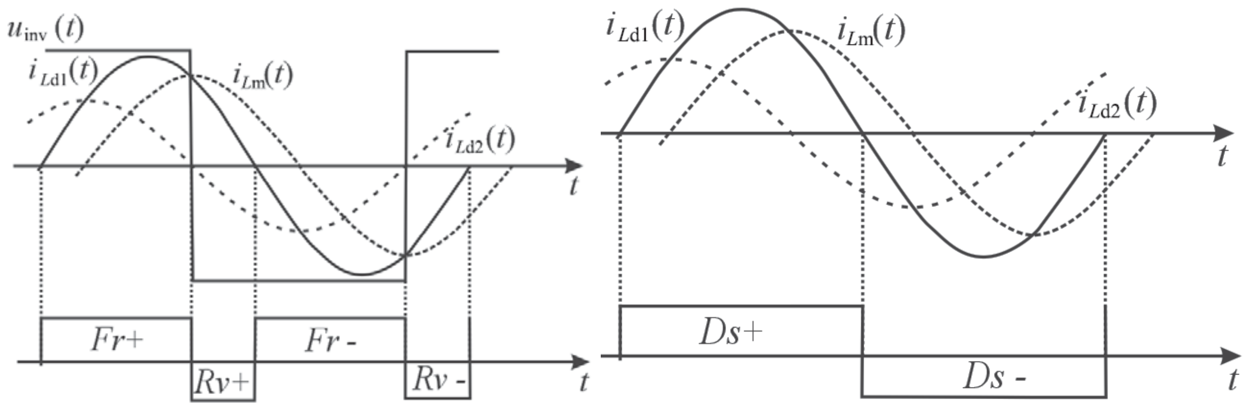

a) b)

Fig. 3. . Conversion phases of the series-to-series RC:
a — energy transfer to the circuit, *b* — dissipation of the energy accumulated in the circuit

Table 1. Equivalent circuits of the series-to-series RC for the conversion phases under consideration

Conversion phase	Resonant current sign	Closed keys	Equivalent circuit
Fr	+	VT2 VT3 VD5 VD8	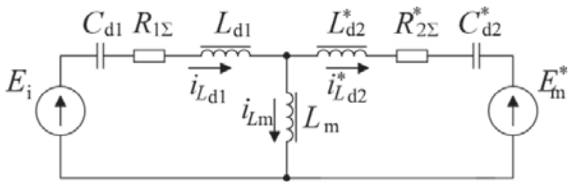
	–	VT1 VT4 VD6 VD7	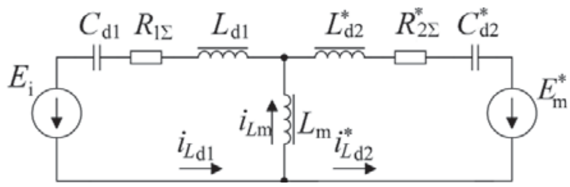
Ds	+	VT3 VT4 VD5 VD8	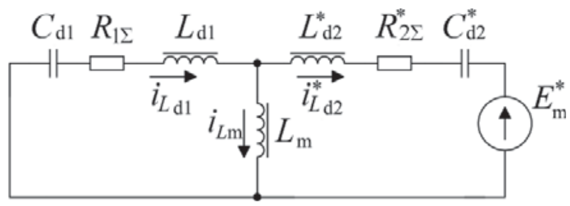
	–	VT3 VT4 VD6 VD7	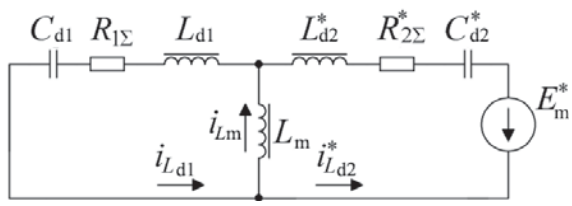
Rv	+	VD1 VD4 VD5 VD8	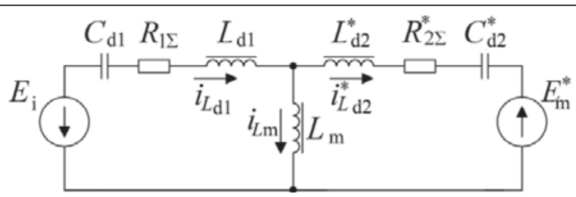
	–	VD2 VD3 VD6 VD7	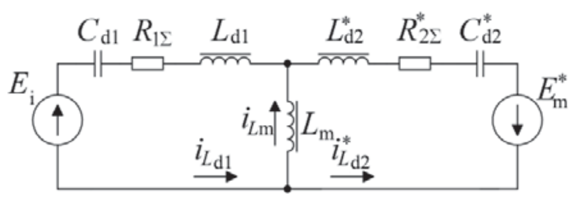

The system of equations describing the processes occurring in the resonant circuit during the positive half-wave of the ***Fr*** conversion phase has the following vector-matrix form:

$$\mathbf{x}(t) = \mathbf{A}_{Fr+} \cdot \mathbf{x}(t) + \mathbf{B}_{Fr+} \cdot \mathbf{E}; \qquad (1)$$

$$y(t) = \mathbf{C}_{Fr+} \cdot \mathbf{x}(t). \qquad (2)$$

The matrices of the coefficients of the system of equations are as follows:

$$\mathbf{A}_{Fr+} = \begin{bmatrix} -\frac{K_{RL}}{K_L} & \frac{L_m R_{\Sigma 2}}{K_L} & -\frac{L_{d2}+L_m}{K_L} & -\frac{L_m}{K_L} \\ \frac{L_{d1}R_{\Sigma 2} - L_{d2}R_{\Sigma 1}}{K_L} & -\frac{L_{d1}R_{\Sigma 2}}{K_L} & -\frac{L_{d2}}{K_L} & \frac{L_{d1}}{K_L} \\ \frac{1}{C_{d1}} & 0 & 0 & 0 \\ \frac{1}{C_{d2}} & -\frac{1}{C_{d2}} & 0 & 0 \end{bmatrix};$$

$$\mathbf{B}_{Fr+} = \begin{bmatrix} \frac{L_{d2}+L_m}{K_L} & -\frac{L_m}{K_L} \\ \frac{L_{d2}}{K_L} & \frac{L_{d1}}{K_L} \\ 0 & 0 \\ 0 & 0 \end{bmatrix}; \quad \mathbf{C}_{Fr+} = \begin{bmatrix} 1 & -1 & 0 & 0 \end{bmatrix},$$

where $K_L = L_{d1}L_{d2} + L_{d1}L_m + L_{d2}L_m$, $K_{RL} = R_{\Sigma 1}L_{d2} + R_{\Sigma 1}L_m + R_{\Sigma 2}L_m$.

The equations for the negative half-wave of the ***Fr*** phase are identical, up to the signs of the EMF values, i.e. $\mathbf{B}_{Fr-} = -\mathbf{B}_{Fr+}$. The following equality is satisfied (also valid for other conversion phases):

$$x(t + T_{osc}/2) = \mathbf{M} \cdot x(t). \qquad (3)$$

where $\mathbf{M} = -\mathbf{I}$, $\mathbf{I}$ is the identity diagonal matrix.

The equations describing the processes occurring in the resonant circuit during the positive half-wave of the resonant current of the ***Rv*** conversion phase have the following vector-matrix form:

$$\mathbf{x}(t) = \mathbf{A}_{Rv+} \cdot \mathbf{x}(t) + \mathbf{B}_{Rv+} \cdot \mathbf{E}; \qquad (4)$$

$$y(t) = \mathbf{C}_{Rv+} \cdot \mathbf{x}(t). \qquad (5)$$

$$\mathbf{A}_{Rv+} = \begin{bmatrix} -\frac{K_{RL}}{K_L} & \frac{L_m R_{\Sigma 2}}{K_L} & -\frac{L_{d2}+L_н}{K_L} & -\frac{L_m}{K_L} \\ \frac{L_{d1}R_{\Sigma 2} - L_{d2}R_{\Sigma 1}}{K_L} & -\frac{L_{d1}R_{\Sigma 2}}{K_L} & -\frac{L_{d2}}{K_L} & \frac{L_{d1}}{K_L} \\ \frac{1}{C_{d1}} & 0 & 0 & 0 \\ \frac{1}{C_{d2}} & -\frac{1}{C_{d2}} & 0 & 0 \end{bmatrix};$$

$$\mathbf{B}_{Rv+} = \begin{bmatrix} -\frac{L_{d2}+L_m}{K_L} & -\frac{L_m}{K_L} \\ -\frac{L_{d2}}{K_L} & \frac{L_{d1}}{K_L} \\ 0 & 0 \\ 0 & 0 \end{bmatrix}; \quad \mathbf{C}_{Rv+} = \begin{bmatrix} 1 & -1 & 0 & 0 \end{bmatrix}.$$

The expression $\mathbf{B}_{Rv-} = -\mathbf{B}_{Rv+}$ is also valid for the negative half-wave.

The system of equations for the positive half-wave of the resonant current of the ***Ds*** conversion phase has the following vector-matrix form:

$$\mathbf{x}(t) = \mathbf{A}_{Ds+} \cdot \mathbf{x}(t) + \mathbf{B}_{Ds+} \cdot \mathbf{E}; \qquad (6)$$

$$y(t) = \mathbf{C}_{Ds+} \cdot \mathbf{x}(t). \qquad (7)$$

where

$$\mathbf{A}_{Ds+} = \begin{bmatrix} -\frac{K_{RL}}{K_L} & \frac{L_m R_{\Sigma 2}}{K_L} & -\frac{L_{m2}+L_m}{K_L} & -\frac{L_m}{K_L} \\ \frac{L_{d1}R_{\Sigma 2} - L_{d2}R_{\Sigma 1}}{K_L} & -\frac{L_{d1}R_{\Sigma 2}}{K_L} & -\frac{L_{d2}}{K_L} & \frac{L_{d1}}{K_L} \\ \frac{1}{C_{d1}} & 0 & 0 & 0 \\ \frac{1}{C_{d2}} & -\frac{1}{C_{d2}} & 0 & 0 \end{bmatrix};$$

$$\mathbf{B}_{Ds+} = \begin{bmatrix} 0 & -\frac{L_m}{K_L} \\ 0 & \frac{L_{d1}}{K_L} \\ 0 & 0 \\ 0 & 0 \end{bmatrix}; \quad \mathbf{C}_{Ds+} = \begin{bmatrix} 1 & -1 & 0 & 0 \end{bmatrix}. \quad \mathbf{B}_{Ds-} = -\mathbf{B}_{Ds+}.$$

Let us introduce the following notations:

$$\mathbf{A}_{Ds+} = \mathbf{A}_{Rv+} = \mathbf{A}_{Fr+} = \mathbf{A}_{Ds-} = \mathbf{A}_{Rv-} = \mathbf{A}_{Fr-} = \mathbf{A}_{SS};$$

$$\mathbf{C}_{Ds+} = \mathbf{C}_{Rv+} = \mathbf{C}_{Fr+} = \mathbf{C}_{Ds-} = \mathbf{C}_{Rv-} = \mathbf{C}_{Fr-} = \mathbf{C}_{SS};$$

$$\mathbf{B}_{Fr-} = -\mathbf{B}_{Fr+} = -\mathbf{B}_{Fr};$$

$$\mathbf{B}_{Rv-} = -\mathbf{B}_{Rv+} = -\mathbf{B}_{Rv};\ \mathbf{B}_{Ds-} = -\mathbf{B}_{Ds+} = -\mathbf{B}_{Ds}.$$

The following functions are the solutions to the vector-matrix differential equations (1), (4), (6):

a) conversion phase ***Fr***, positive half-wave ($kT_{osc} < t < t_{Fr+}$):

$$\mathbf{x}(t) = e^{\mathbf{A}_{SS}(t - kT_{osc})} \cdot \mathbf{x}(kT_{osc}) + \mathbf{D}_{SS}(t - kT_{osc}) \cdot \mathrm{B}_{Fr} \cdot \mathbf{E}; \quad (8)$$

b) conversion phase ***Fr***, negative half-wave ($(k+1/2)\,T_к < t < t_{Fr-}$):

$$\mathbf{x}(t) = e^{\mathbf{A}_{SS}(t-(k+\frac{1}{2})T_{osc})} \cdot \mathbf{x}((k+\frac{1}{2})T_{osc}) - \\ - \mathbf{D}_{SS}(t-(k+\frac{1}{2})T_{osc}) \cdot \mathrm{B}_{Fr} \cdot \mathbf{E}; \qquad (9)$$

c) conversion phase ***Rv***, positive half-wave ($kT_{osc} + t_{Fr+} < t < (k+1/2)T_к$):

$$\mathbf{x}(t) = e^{\mathbf{A}_{SS}(t - kT_{osc} + t_{Fr})} \cdot \mathbf{x}(kT_{osc} + t_{Fr}) + \\ + \mathbf{D}_{SS}(t - kTosc - t_{Fr}) \cdot \mathbf{B}_{Rv} \cdot \mathbf{E}; \qquad (10)$$

d) conversion phase ***Rv***, negative half-wave ($(k+1/2)T_{osc} + t_{Fr+} < t < kT_{osc}$):

$$\mathbf{x}(t) = e^{\mathbf{A}_{SS}(t-(k+\frac{1}{2})T_{osc} - t_{Fr})} \cdot \mathbf{x}((k+\frac{1}{2})T_{osc} + t_{Fr}) - \\ - \mathbf{D}_{SS}(t-(k+\frac{1}{2})T - t_{Fr}) \cdot \mathbf{B}_{Rv} \cdot \mathbf{E}; \qquad (11)$$

e) conversion phase ***Ds***, positive half-wave ($(k+n_{FrRv}) \cdot T_{osc} < t < (k+1/2+n_{FrRv}) \cdot T_{osc}$):

$$\mathbf{x}(t) = e^{\mathbf{A}_{SS}(t-(k+n_{FrRv})\cdot\frac{T_{\text{osc}}}{2})} \cdot \mathbf{x}((k+n_{FrRv})\cdot\frac{T_{\text{osc}}}{2}) +$$

$$+\mathbf{D}_{SS}(t-(k+n_{FrRv})\cdot\frac{T_{\text{osc}}}{2})\cdot\mathbf{B}_{Ds}\cdot\mathbf{E}; \qquad (12)$$

f) conversion phase ***Ds***, negative half-wave $((k+1/2+n_{FrRv})\cdot T_{\text{osc}}<t<(k+1+n_{FrRv})\cdot T_{\text{osc}})$:

$$\mathbf{x}(t) = e^{\mathbf{A}_{SS}(t-(k+1+n_{FrRv})\cdot\frac{T_{\text{osc}}}{2})} \cdot \mathbf{x}((k+1+n_{FrRv})\cdot\frac{T_{\text{osc}}}{2}) -$$

$$-\mathbf{D}_{SS}(t-(k+1+n_{FrRv})\cdot\frac{T_{\text{osc}}}{2})\cdot\mathbf{B}_{Ds}\cdot\mathbf{E}, \qquad (13)$$

where

$$\mathbf{D}_{SS} = \int_0^t e^{\mathbf{A}_{SS}(t-\psi)}d\psi = \mathbf{A}_{SS}^{-1}\cdot(\mathbf{I}-e^{\mathbf{A}_{SS}t}); \qquad (14)$$

I is the identity diagonal matrix.

The average output current for the half-cycle of the circuit loading (***Fr***, ***Rv*** phases) can be calculated as follows:

$$y_{av}(0) = \frac{2}{T_{\kappa}}\int_0^{T_{osc}/2} y(t)dt = \frac{2}{T_{osc}}\mathbf{C}_{SS}[\int_0^{t_{Fr}}\mathbf{x}(t)dt + \int_{t_{Fr}}^{T_{osc}/2}\mathbf{x}(t)dt]; \quad (15)$$

$$y_{av}(0) = \mathbf{C}_1\cdot x(0) + \mathbf{D}_1\cdot\mathbf{E}, \qquad (16)$$

where

$$\mathbf{C}_1 = -\frac{2}{T_{osc}}\mathbf{C}_{SS}\{\mathbf{D}_{SS}(t_{Fr}) + e^{\mathbf{A}_{SS}t_{Fr}}\cdot\mathbf{D}_{SS}(T_{osc}/2-t_{Fr1})\}; \quad (17)$$

$$\mathbf{D}_1 = \frac{2}{T_{osc}}\mathbf{C}_{SS}\{\mathbf{A}_{SS}^{-1}\cdot[\mathbf{D}_{SS}(t_{Fr1}) + I\cdot t_{Fr1}]\cdot \mathrm{B}_{Fr} -$$

$$-\mathbf{D}_{SS}(T_{osc}/2-t_{Fr1})\cdot\mathbf{D}_{SS}(t_{Fr1})\cdot \mathrm{B}_{Fr} +$$

$$+\mathbf{A}_{SS}^{-1}\cdot\{\mathbf{D}_{SS}(T_{osc}/2-t_{Fr}) + I\cdot(T_{osc}/2-t_{Fr})\}\cdot\mathbf{B}_{Rv}\}. \quad (18)$$

The average output current for the negative half-cycle can be written as follows:

$$y_{av}(0) = \mathbf{C}_1\cdot x(0) - \mathbf{D}_1\cdot\mathbf{E}.$$

The average output current for the energy dissipation half-cycle of the (***Ds*** phase) can be calculated in the following way:

$$y_{av}(0) = \frac{2}{T_{osc}}\int_0^{T_{osc}/2} y(t)dt = \frac{2}{T_{osc}}\mathbf{C}_{SS}\cdot\int_0^{T_{osc}/2}\mathbf{x}(t)dt; \qquad (19)$$

$$y_{av}(0) = \mathbf{C}_2\cdot x(0) + \mathbf{D}_2\cdot\mathbf{E}, \qquad (20)$$

where

$$\mathbf{C}_2 = -\frac{2}{T_{osc}}\mathbf{C}_{SS}\mathbf{D}_{SS}(T_{osc}/2); \qquad (21)$$

$$\mathbf{D}_2 = \frac{2}{T_{osc}}\mathbf{C}_{SS}\mathbf{A}_{SS}^{-1}\cdot[\mathbf{D}_{SS}(T_{osc}/2) + I\cdot T_{osc}/2]\cdot \mathrm{B}_{Ds}. \quad (22)$$

The average output current in the negative half-cycle can be written as follows:

$$y_{av}(0) = \mathbf{C}_2\cdot x(0) - \mathbf{D}_2\cdot\mathbf{E}.$$

These expressions describe the electromagnetic processes in the power section of the series-to-series RC within one half-cycle.

Substituting actual parameters of the converter to the obtained expressions, one can calculate the adjustment and loading characteristics of the series-to-series RC by means of numerical simulation. To bring static characteristics to the dimensionless form, the following coefficients are introduced:

$$q_E = \frac{E_{\text{m}}}{E_{\text{m}}};\ q_I = \frac{I_{\text{m}}}{I_{\text{m.max}}},$$

where $I_{\text{m.max}}$ is the maximum calculated output current. When charging a battery, this current must be equal to or greater than the rated charging current $I_{\text{m.rated}}$ determined by the battery's capacity. For example, a battery with the capacity of 2500 mA/h corresponds to $I_{\text{m.rated}}$ = 2500 mA. The voltage at the battery terminals most often varies within q_E = 0.5...0.7 from the source voltage [5].

Fig. 4 demonstrates the groups of adjustment characteristics of a series-to-series RC with an air gap of 250 mm (*a*) and 45 mm (*b*).

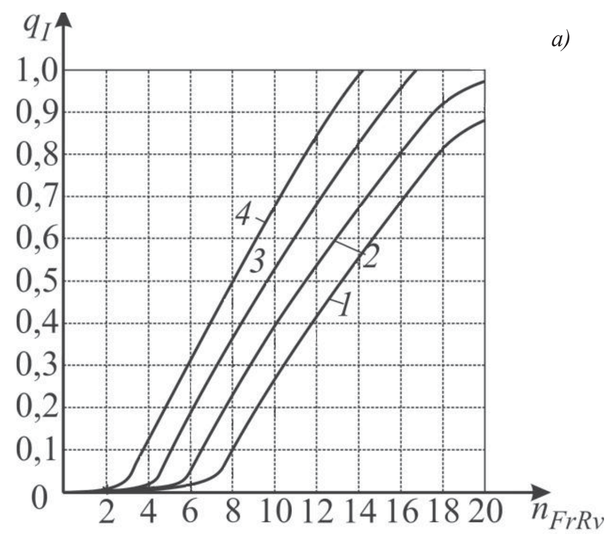

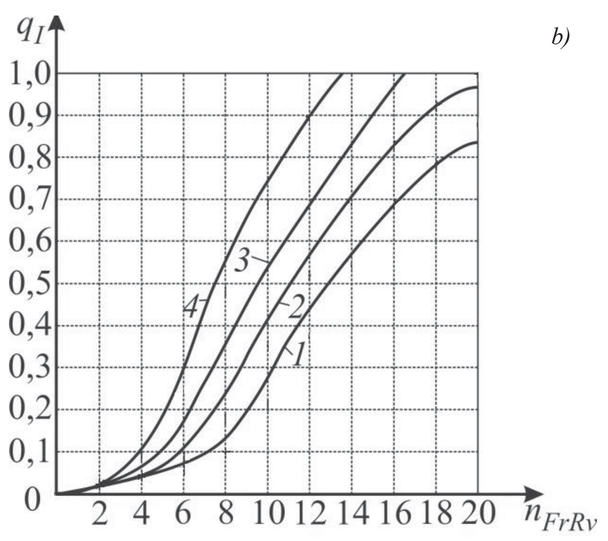

Fig. 4. Adjustment characteristics of a series-to-series RC:
a — with an air gap of 250 mm; *b* — 45 mm;
1 — q_E = 0.8; 2 — q_E = 0.7; 3 — q_E = 0.6; 4 — q_E = 0.5

The adjustment characteristics at the gap of 250 mm are virtually linear, whereas at 45 mm they acquire a non-linearity in the area of small values of nFrRv. The output current is substantially affected by the load's anti-EMF. The dependence of the output current on the magnitude of the anti-EMF is more clearly illustrated by the group of curves shown in Fig. 5.

The converter has the properties of a constant voltage source. For battery charging, it must be designed with the average output current being equal to at the maximum anti-EMF load and control value. With an air gap close to zero, the characteristics of the series-to-series RC will be similar to those of the series RC with relay control [1].

CONCLUSIONS. The article analyzes the electromagnetic processes in the power section of a series-to-series resonant converter for contactless inductive energy transfer. The processes are presented by dividing the conversion half-cycles into the transformation phases. Upon solving the vector-matrix systems of equations describing the electromagnetic processes in the power section of the RC for WIET, it was possible to obtain an analytical expression for the average output current of the converter. It depends on the parameters of the elements of the resonant circuits, the size of the air gap of the converter, the source and load parameters. The obtained dependences can be applied to calculate the adjustment and load characteristics of a series-to-series RC by means of numerical simulation with regard to actual parameters of the converter.

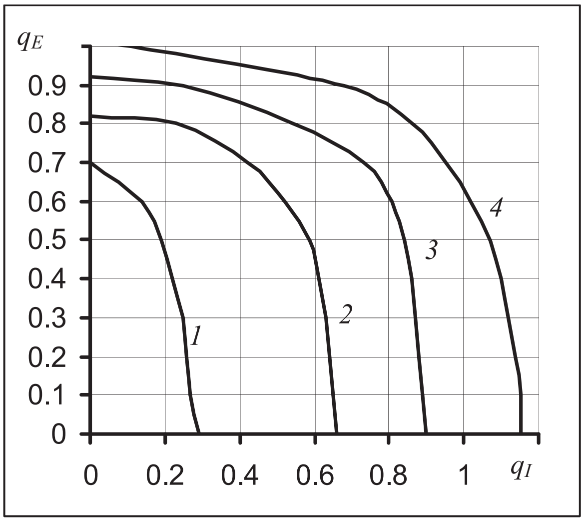

Fig. 5. Dependences of the output current of a series-to-series RC on the load's anti-EMF at the air gap of 250 mm: *1* — $n_{FrRv} = 5$; *2* — $n_{FrRv} = 10$; *3* — $n_{FrRv} = 15$; *4* — $n_{FrRv} = 20$

Статью рекомендует в печать
д-р техн. наук, проф. *В. М. Рябенький*